PHASE DIAGRAM AND ISENTROPIC CURVES FROM THE VECTOR MESON EXTENDED POLYAKOV QUARK MESON MODEL*

Péter Kovács, György Wolf

Institute for Particle and Nuclear Physics, Wigner Research Centre for Physics
Hungarian Academy of Sciences, Budapest, Hungary

(Received August 21, 2017)

In the framework of the $N_\mathrm{f} = 2+1$ flavor (axial)vector meson extended Polyakov quark meson model, we investigate the QCD phase diagram at finite temperature and density. We use a χ^2 minimization procedure to parameterize the model based on tree-level decay widths and vacuum scalar and pseudoscalar curvature masses which incorporate the contribution of the constituent quarks. Using a hybrid approximation (mesons at tree level, fermions at one-loop level) for the grand potential, we determine the phase boundary both on the μ_B–T and ρ–T planes. We also determine the location of the critical end point of the phase diagram. Moreover, by calculating the pressure and other thermodynamical quantities derived from it, we determine a set of isentropic curves in the crossover region. We show that the curves behave very similarly as their counterparts obtained from the lattice in the crossover regime.

DOI:10.5506/APhysPolBSupp.10.1107

1. Introduction

Our understanding of the properties of the strongly interacting matter can be greatly improved with the upcoming FAIR facility in the sense that investigation of a different region and might be the location of the critical end point (CEP), if it exists at all, becomes available. However, for the experiments, better and better theoretical predictions are also necessary.

With the help of a vector/axial vector extended Polyakov quark meson model, which was already described in [1], we further analyze some aspects of the chiral phase transition. In the present approximation, our model contains a scalar, a pseudoscalar, a vector and an axial vector nonet field, beside the u, d, s constituent quarks. It is important to note the existence of a particle assignment ambiguity in the scalar sector, namely, there are more physical fields below 2 GeV in the scalar sector than we can describe with

* Presented at "Excited QCD 2017", Sintra, Lisbon, Portugal, May 7–13, 2017.

one scalar nonet. Thus, one has to try different assignments — there are 40 possibilities — during the determination of the Lagrangian parameters and see which one is the best (for more detail, see Sec. 3 and [1,2]). With the best set of parameters, one can solve — with some further approximations — the field equations at finite temperature T and/or baryon chemical potential $\mu_{\rm B}$.

From that solution, the phase boundary and $T/\mu_{\rm B}$ dependence of various physical quantities are readily given.

The paper is organized as follows. In Sec. 2, the model is introduced with its Lagrangian. Here the field equations, which determine the temperature and baryochemical potential dependence of the order parameters, are also presented. The parameterization is briefly described in Sec. 3, followed by the results in Sec. 4 showing the phase boundary and a set of isentropic curves compared with their lattice counterpart. Finally, we conclude in Sec. 5.

2. The model and the field equations

The model is described by the following Lagrangian, which can be found in more detail in [1,2]:

$$\begin{aligned}\mathcal{L} = {} & \mathrm{Tr}\left[(D_\mu M)^\dagger (D_\mu M)\right] - m_0^2\,\mathrm{Tr}\left(M^\dagger M\right) - \lambda_1\left[\mathrm{Tr}\left(M^\dagger M\right)\right]^2 \\ & -\lambda_2\,\mathrm{Tr}\left(M^\dagger M\right)^2 + c_1\left(\det M + \det M^\dagger\right) + \mathrm{Tr}\left[H\left(M+M^\dagger\right)\right] \\ & -\frac{1}{4}\,\mathrm{Tr}\left(L_{\mu\nu}^2 + R_{\mu\nu}^2\right) + \mathrm{Tr}\left[\left(\frac{m_1^2}{2}+\Delta\right)\left(L_\mu^2+R_\mu^2\right)\right] \\ & +i\frac{g_2}{2}\left(\mathrm{Tr}\{L_{\mu\nu}\left[L^\mu,L^\nu\right]\} + \mathrm{Tr}\{R_{\mu\nu}[R^\mu,R^\nu]\}\right) \\ & +\frac{h_1}{2}\,\mathrm{Tr}\left(M^\dagger M\right)\mathrm{Tr}\left(L_\mu^2+R_\mu^2\right) + h_2\,\mathrm{Tr}\left[(L_\mu M)^2 + (MR_\mu)^2\right] \\ & +2h_3\,\mathrm{Tr}\left(L_\mu M R^\mu M^\dagger\right) + \bar{\Psi}\left[i\gamma_\mu D^\mu - g_{\rm F}\left(\mathbb{1}_{4\times4}M_{\rm S} + i\gamma_5 M_{\rm PS}\right)\right]\Psi\,, \quad (1)\end{aligned}$$

with $M \equiv M_{\rm S}+M_{\rm PS}$ being the scalar–pseudoscalar nonet fields, $L^\mu \equiv V^\mu + A^\mu$, $R^\mu \equiv V^\mu - A^\mu$ stand for the left- and right-handed vector nonets (which are linear combinations of the V^μ vector and A^μ axial vector nonet physical fields), the external fields are defined as $H = \frac{1}{2}\mathrm{diag}(h_{0\rm N}, h_{0\rm N}, \sqrt{2}h_{0\rm S})$ and $\Delta = \mathrm{diag}(\delta_{\rm N}, \delta_{\rm N}, \delta_{\rm S})$, while $G^\mu = g_s G_i^\mu T_i$[1] are the gluon fields.

As a usual process, we use the spontaneous symmetry breaking scenario with two non-zero vacuum expectation values denoted by $\phi_{\rm N}$ and $\phi_{\rm S}$ — connected to the $\lambda_{\rm N} = \frac{1}{\sqrt{3}}(\sqrt{2}\lambda_0 + \lambda_8)$ non-strange and $\lambda_{\rm S} = \frac{1}{\sqrt{3}}(\lambda_0 - \sqrt{2}\lambda_8)$ strange generators in the scalar sector.

[1] Here, $T_i = \lambda_i/2$ $(i = 1,\ldots,8)$ denote the SU(3) group generators, with the λ_i Gell-Mann matrices.

In the present mean-field-approximation, we assume non-vanishing gluon field only in the temporal direction (G^4), which is additionally assumed to be x-independent and diagonal in color space. This will give rise to the Polyakov loop variables Φ and $\bar{\Phi}$, when calculating the partition function $\mathcal{Z}$ on the constant gluon background G^4 (see details in [1]). For the Polyakov-loop potential, we use an improved logarithmic potential (proposed in [3]), which takes into account some part of the gluon dynamics.

The grand potential Ω is calculated by taking into account only the fermionic fluctuations and treating the mesons at tree-level. Consequently, the grand potential has four parts, which are the classical mesonic potential, the Polyakov-loop potential, the fermionic vacuum and thermal parts

$$\Omega(T,\mu_q) = U_{\rm mes}(\phi_{\rm N},\phi_{\rm S}) + U_{\rm Pol}\left(\Phi,\bar{\Phi}\right) + \Omega_{\bar{q}q}^{(0){\rm vac}} + \Omega_{\bar{q}q}^{(0)T}(T,\mu_q)\,. \tag{2}$$

Here, $\mu_q = \mu_{\rm B}/3$ and not every variable dependence is explicitly shown.

The values of the order parameters — as a function of T,μ_q — are obtained from the four coupled field equations

$$\frac{\partial\Omega}{\partial\phi_{\rm N}} = \frac{\partial\Omega}{\partial\phi_{\rm S}} = \frac{\partial\Omega}{\partial\Phi} = \frac{\partial\Omega}{\partial\bar{\Phi}} = 0\,. \tag{3}$$

The detailed form of the field equations can be found in [1].

3. Parameterization

To solve Eq. (3) — the set of coupled field equations — one has to determine the 14 unknown parameters (m_0, λ_1, λ_2, c_1, $m_1+\phi_{\rm N}$, h_1, h_2, h_3, $\delta_{\rm S}$, $\phi_{\rm N}$, $\phi_{\rm S}$, $g_{\rm F}$, g_1, g_2) of Eq. (1) Lagrangian. Therefore, we calculate a set of observables at zero temperature (at tree-level: 5 vector/axial vector masses, 2 constituent quark masses, 12 decay width, 2 PCAC relations, at one-loop level: 8 scalar/pseudoscalar curvature masses) and compare with their PDG values [4] through a multiparametric χ^2 minimalization procedure [5]. Beside the zero temperature quantities, we also use the pseudocritical temperature $T_{\rm c}$ at $\mu_{\rm B}=0$ and compare with its lattice result taken from [6]. It is worth to note that the errors of the observables used for the χ^2 minimalization are set to 20% for the scalar masses and their decay widths, 10% for the constituent quarks and the $T_{\rm c}$, and 5% for the remaining quantities as long as their PDG errors are not larger (in that case, we use the PDG error). We started the parameterization procedure from 5×10^4 points in the parameter space for the different assignment scenarios of the scalar sector, and chose that gave the minimal χ^2 value. The resulting parameters and further details can be found in [1].

4. Results: chiral phase boundary and isentropic curves

Once Eq. (3) is solved, the points of the phase boundary are given by the inflection points of the $\phi_{\rm N}(T)$ curve for different values of $\mu_{\rm B}$. When solving the field equations, we also calculate the grand canonical potential $\Omega(T,\mu_q)$ along the solution from which the pressure is simply given by

$$p(T,\mu_q) = \Omega(T=0,\mu_q) - \Omega(T,\mu_q)\,, \tag{4}$$

while the entropy and quark number densities are defined as $s = \partial p/\partial T$, and $\rho_q = \partial p/\partial \mu_q$, respectively. The phase diagram is shown in Fig. 1 on the T–$\mu_{\rm B}$ plane together with the chemical freezout curve. On the phase boundary, a second order critical end point — which separates the crossover and the first order regimes — exists at $(\mu_{\rm B}, T) = (885, 53)$ MeV. In the inset of Fig. 1, the variation of the location of the CEP with the f_0 mass is shown.

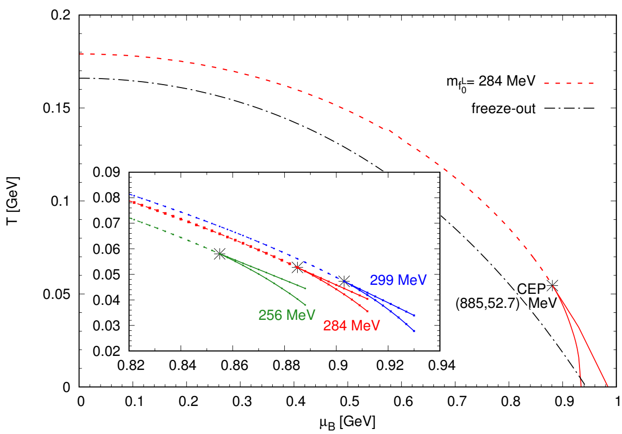

Fig. 1. Phase diagram on the T–$\mu_{\rm B}$ plane.

If instead of the baryochemical potential we use the $\rho_{\rm B} = \rho_q/3$ baryon density, we get the phase boundary on the T–$\rho_{\rm B}$ plane (Fig. 2), where the baryon density is normalized with the normal nuclear density $\rho_0 = 0.16\frac{1}{{\rm fm}^3}$. Here, the two curves correspond to two different Polyakov-loop potential presented in [7] (upper curve) and [1] (lower curve). We find that the phase boundary curves have a very similar shape found by others (see *e.g.* [8]). However, our CEP is located at a lower $\rho_{\rm B}/\rho_0$ value than in [8], where the CEP was located at $\rho_{\rm B}/\rho_0 \approx 2$ in a PNJL model calculation.

It is also interesting to investigate the isentropic curves on the T–$\mu_{\rm B}$ plane, which is defined as $S/N = s/\rho_q = {\rm const}$. These curves can be determined on the lattice as well. Our curves are shown on Fig. 3, while the lattice version, which uses analytic continuation to the finite $\mu_{\rm B}$ region is depicted in Fig. 4 [9].

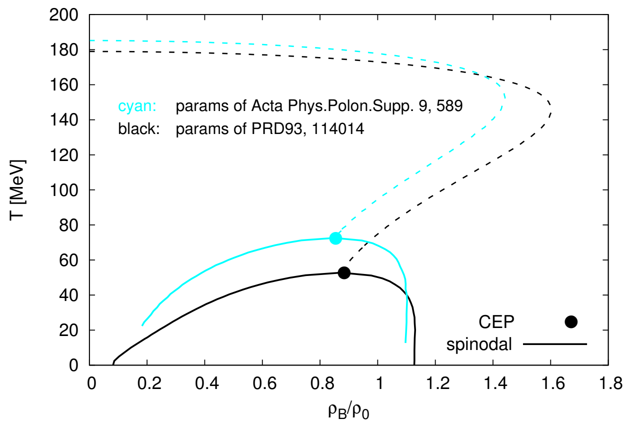

Fig. 2. Phase diagram on the T–ρ_B plane.

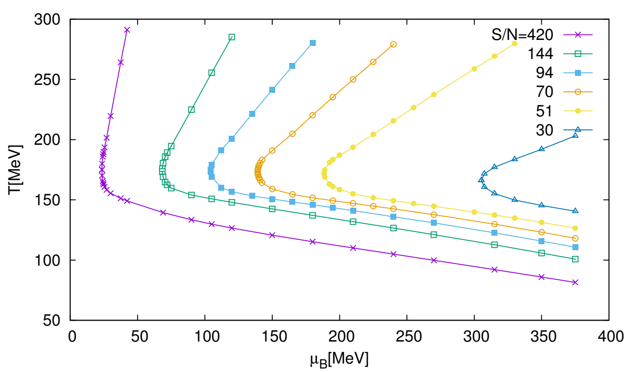

Fig. 3. The calculated isentropic curves for different values of S/N.

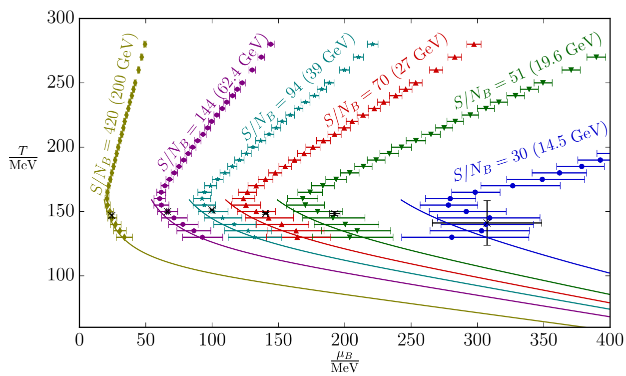

Fig. 4. Isentropic curves from lattice for different values of S/N from [9].

The two sets of curves coincide very well. Since our curves are in the crossover region and it is known — from *e.g.* [8] — that in the first order region the curves looks differently (always have some 'S'-shaped part), we can conclude that in the $\mu_{\mathrm{B}} < 400$ MeV region the existence of a CEP is unlikely on the lattice.

5. Conclusion

In the framework of an (axial)vector Polyakov quark meson model some aspects of the in-medium properties of the strongly interacting matter was presented. The calculated isentropic curves in the crossover regime show a very good agreement with the corresponding curves on the lattice. This suggests a large baryochemical potential value ($\mu_{\mathrm{B,CEP}} > 400$ MeV) at the CEP on the lattice.

To improve our model, mesonic fluctuations and additional fields like four-quark states could be included.

The authors were supported by the Hungarian OTKA fund K109462 and by the HIC for FAIR Guest Funds of the Goethe University Frankfurt. The authors thank Zs. Szép for making figures.

REFERENCES

[1] P. Kovács, Zs. Szép, Gy. Wolf, *Phys. Rev. D* **93**, 114014 (2016).

[2] D. Parganlija *et al.*, *Phys. Rev. D* **87**, 014011 (2013).

[3] L.M. Haas *et al.*, *Phys. Rev. D* **87**, 076004 (2013).

[4] K.A. Olive *et al.* [Particle Data Group], *Chin. Phys. C* **38**, 090001 (2014).

[5] F. James, M. Roos, *Comput. Phys. Commun.* **10**, 343 (1975).

[6] Y. Aoki, Z. Fodor, S.D. Katz, K.K. Szabo, *Phys. Lett. B* **643**, 46 (2006).

[7] Zs. Szép, P. Kovács, Gy. Wolf, *Acta Phys. Pol. B Proc. Suppl.* **9**, 589 (2016).

[8] P. Costa, *Phys. Rev. D* **93**, 114035 (2016).

[9] Günther *et al.*, *EPJ Web Conf.* **137**, 07008 (2017) [`arXiv:1607.02493 [hep-lat]`].